Facies analysis and diagenetic evolution of the Dinantian carbonates in the Dutch subsurface: data and analyses well KSL-02

Report by SCAN

October 2019

Ministerie van Economische Zaken en Klimaat
ebn
TNO
Interreg North-West Europe DGE-ROLLOUT

Facies analysis and diagenetic evolution of the Dinantian carbonates in the Dutch subsurface: data and analyses well KSL-02

Written by:
Mahtab Mozafari[1], Peter Gutteridge[2], Alberto Riva[3], Kees Geel[4], Joanna Garland[2] and Julie Dewit[2]

October 2019

1- Energie Beheer Nederland (EBN), Daalsesingel 1, 3511 SV Utrecht, the Netherlands
2- Cambridge Carbonates Ltd, No. 4 The Courtyard, 707 Warwick Road, Solihull, B91 3DA, UK
3- G.E.Plan Consulting srl, Via L. Ariosto 58, 44121 Ferrara, Italy
4- Geological Survey of the Netherlands (TNO), Princetonlaan 6, 3584 CB Utrecht, the Netherlands

Dit rapport is een product van het SCAN-programma en wordt mogelijk gemaakt door het Ministerie van Economische Zaken en Klimaat

Table of contents

6. Kastanjelaan 02 (KSL-02)

6.1 Introduction

The KSL-02 is located in the western Maastricht area, SE Netherlands, very close to the Kastanjelaan-DB123 (KSL-DB123) well (Figures 6-1 and 6-2, Tables 6-1 and 6-2). The KSL-02 well was drilled in 1981, reaching a depth of 500.50 m. The well had a lot of issues during drilling due to the instability of the borehole, that led to the lowering of the casing twice (to 357.30 m and 362.60 m) and injection of cement between 350 and 375 m. The coring was problematic above 380 m, while below it was excellent (95/100 % recovery). The purpose of the well was for mineral water exploration, but the produced water was too saline (10 g/l).

Figure 6-1: Map showing all the wells penetrating the Dinantian carbonates. Location of the KSL-02 well is indicated by red dashed circle.

Figure 6-2: Map showing location of the KSL-02 well (red circle).

Table 6-1: Coordinates and depth of KSL-02 well (from www.nlog.nl).

Co-ordinates (x, y in utm31, ed50 format)	688690, 5637468
Lat/Long (°)	50.85704529, 5.68089962
Supplied co-ordinates	175595, 318530 (RD)
Depth in meters referred to :	Rotary Table
Total depth (m, along hole) :	501
Vertical position of Rotary Table :	58 meter relative to NAP
Trajectory shape :	Vertical
Deviation in X-direction :	0
Deviation in Y-direction :	0
True vertical depth (TVD) in m :	501

Table 6-2: Drilling data about KSL-02 well (from www.nlog.nl).

Client name :	PWL
Start date	Jun 1, 1981
End date	Sep 1, 1981
Drilling company :	Gruner, R., Sittard
Type of well :	Exploration for mineral water
Result :	Mineral water
Status :	Closed

6.2 Available dataset

The majority of the documents on the KSL-02 well are available on "www.nlog.nl" within the following link:
https://www.nlog.nl/nlog/requestData/nlogp/allBor/metaData.jsp?tableName=BorLocation&id=106519265
The most relevant publications/reports used in this study are are as following:

Bless, M. J. M., Bouckaert, J., Bouzet, P., Conil, R., Cornet, P., Fairon-Demaret, M., Groessens, E., Longerstaey, P., Meesen, J. P. M. T., Paproth, E., Pirlet, H., Streel, M., Amerom, H. W. J. and Wolf, M. (1976). Dinantian rocks in the subsurface north of the Brabant and Ardenno- Rhenish massifs in Belgium, the Netherlands and the Federal Republic of Germany. Mededelingen Rijks Geologische Dienst, nieuwe serie, 27, 81-195.

Bless, M. J. M., Boonen, P., Bouckaert, J., Brauckmann, C., Conil, R., Dusar, M., felder, P. J., Felder, W. M., Gökdag, H., Kockel, F., Laloux, M., Langguth, H. R., Van der Meer Mohr, C. G., Meessen, J. P. M. TH., Op het Veld, F., Paproth, E., Pietzner, H., Plum, J., Poty, E., Scherp, A., Schulz, R., Streel, M., Thorez, J., Van Rooijen, P., Vanguestaine, M., Vieslet, J. L., Wiersma, D. J., Winkler Prins, C. F., and Wolf, M. (1981). Preliminary report on Lower Tertiary-Upper Cretaceous and Dinantian-Famennian rocks in the boreholes Heugem-1/1a and Kastanjelaan-2 (Maastricht, the Netherlands). Medelingen Rijks Geologische Dienst, 35, 333-415.

Bless, M. J. M., Bouckaert, J., and Paproth, E. (1981). Vise-Puth: stimulant for further exploration. Annales de La Société Géologique de Belgique, 104, 291-296.

Bless, M. J. M., Bouckaert, J., and Paproth, E. (1983). Recent exploration in pre-Permian rocks around the Brabant Massif in Belgium, the Netherlands and the Federal Republic of Germany. Geologie En Mijnbouw, 62, 51-62.

Friedrich, G., Bless, M. J. M., Vogtmann, J., and Wiechowski, A. (1987). Lead-zinc mineralization in Dinantian rocks of boreholes Thermae 2000 and Thermae 2002 (Valkenburg A/D Geul, The Netherlands). Annales de La Societe Geologique de Belgique, 110, 59-75.

Laenen, B. (2003). Lithostratigrafie van het pre-Tertiair in Vlaanderen. Deel II: Dinantiaan and Devoon. Vito Report.

Poty, E. (1991). Tectonique de blocs dans le prolongement oriental du Massif du Brabant. Annales de La Société Géologique de Belgique, 114, 265-275. Retrieved from http://popups.ulg.ac.be/0037-9395/index.php?id=1479

Poty, E., and Delculée, S. (2011). Interaction between eustacy and block-faulting in the Carboniferous of the Visé – Maastricht area (Belgium, The Netherlands). Zeitschrift Der Deutschen Gesellschaft Für Geowissenschaften, 162, 117-126. https://doi.org/10.1127/1860-1804/2011/0162-0117

TNO. (1999). Toelichting bij Kaartblad XV Silfard-Maastricht. Geologische Atlas van de Diepe Ondergrond van Nederland.

Van Tongeren, P. C. H. (2006). De Vlaamse Voerstreek: een geologische analyse van het Laat Paleozoïcum van deze regio en van het direct aangrenzend gebied (Vol. 2005/MAT/R).

6.2.1 Logs

The available logs were in paper format and were digitised within the framework of the SCAN project.

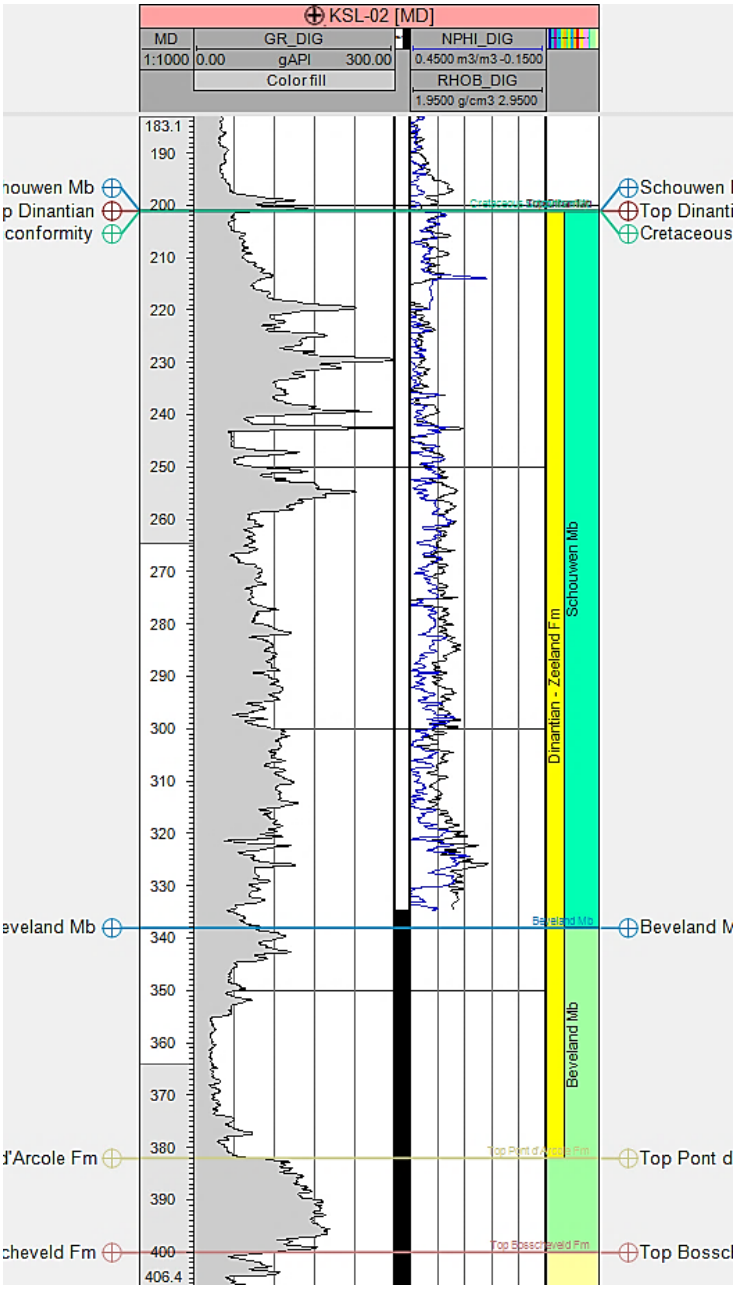

Figure 6-3: Gamma-ray log in the KSL-02 well, with the indication of the cored section (black bar) and the updated biostratigraphy.

6.2.2 Cores, sidewall cores and cuttings

The KSL-02 well was cored for 157 m of continuous succession representative of the lower part of Dinantian and Upper Devonian, from 334.7 until 491.75 m. The recovery is variable, but generally high.

6.2.3 Petrography and additional analyses

TNO provided forty-four thin sections which were described within the framework of this project. In addition, five samples of the KSL-02 core were selected for further diagenetic analysis. New polished thin sections were made for cathodoluminescence petrography (CL) (Table 6-4).
Three thin sections descriptions can be found in Bless et al. (1981).
The following analyses were also available for the KSL-02 well:

- Chemical analyses with calcimetry (seven samples). Some more complete elemental analyses are reported in Bless et al. (1981).
- XRD (four samples) (Figure 6-4).
- Total and Organic carbon (22 samples) (Figure 6-5).
- Vitrinite reflectance (five samples) (Figure 6-5).

Table 6-3: XRD data (Bless et al., 1981).

239.80 m	(GLA 18174): Quartz, illite-sericite' pyrite' kaolinite. dolomite, feldspar
349.45 m	(GLA 18175): Dolomite. Quartz, pyrite, Calcite (rare), illite (rare)
427.95 m	(GLA 18176): Calcite quartz, illite-sericite chlorite, pyrite, dolomite' feldspar' siderite
477.7 m	(GLA 18177) Quartz, calcite, sericite, illite, pyrite, dolomite, feldspar, apatite (?)

In addition to the five new thin sections, stable isotope and fluid inclusion samples were also selected from the same samples. Table 6-4 lists the additional data that were acquired as part of the SCAN project.

Table 6-4: Overview of the samples selected for further analysis.

Sample	**Main diagenetic phase**	**CL**	**Stable isotope sample(s)**	**Fluid inclusions**
338.65 m	Calcite (C3)	+	calcite vein	
351.20 m	Dolomite (D2)	+	dolomite matrix + dolomite vein	
364.40 m	Dolomite (D2)	+		
366.55 m	Dolomite (D2)	+	dolomite matrix + dolomite vein	+
378.40 m	Calcite (C3)	+	calcite matrix + calcite vein	

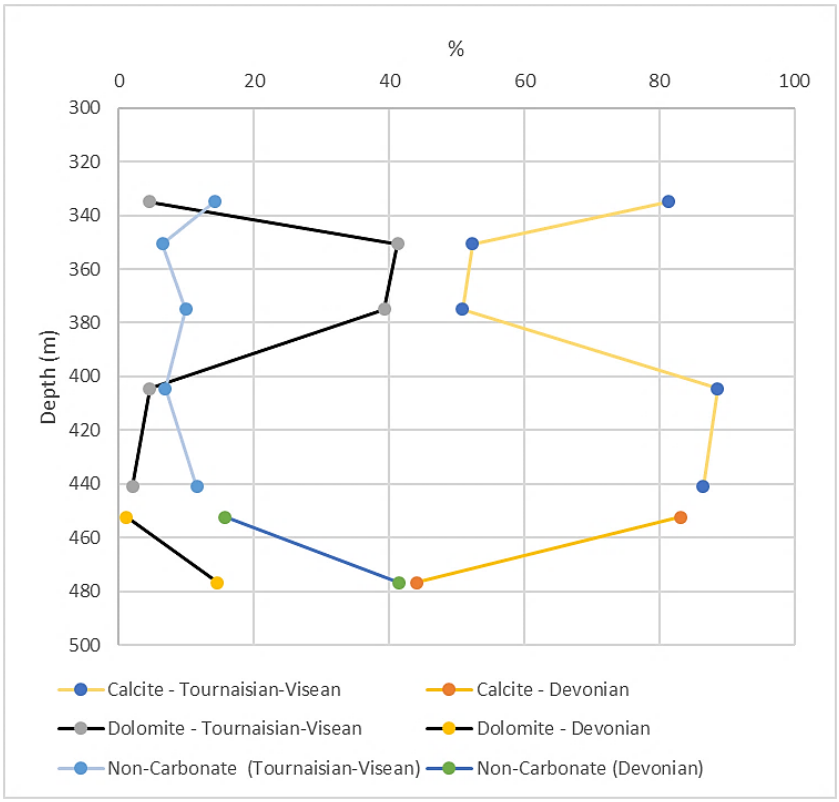

Figure 6-4: Chemical analyses on the KSL-02 well samples (from Bless et al., 1981).

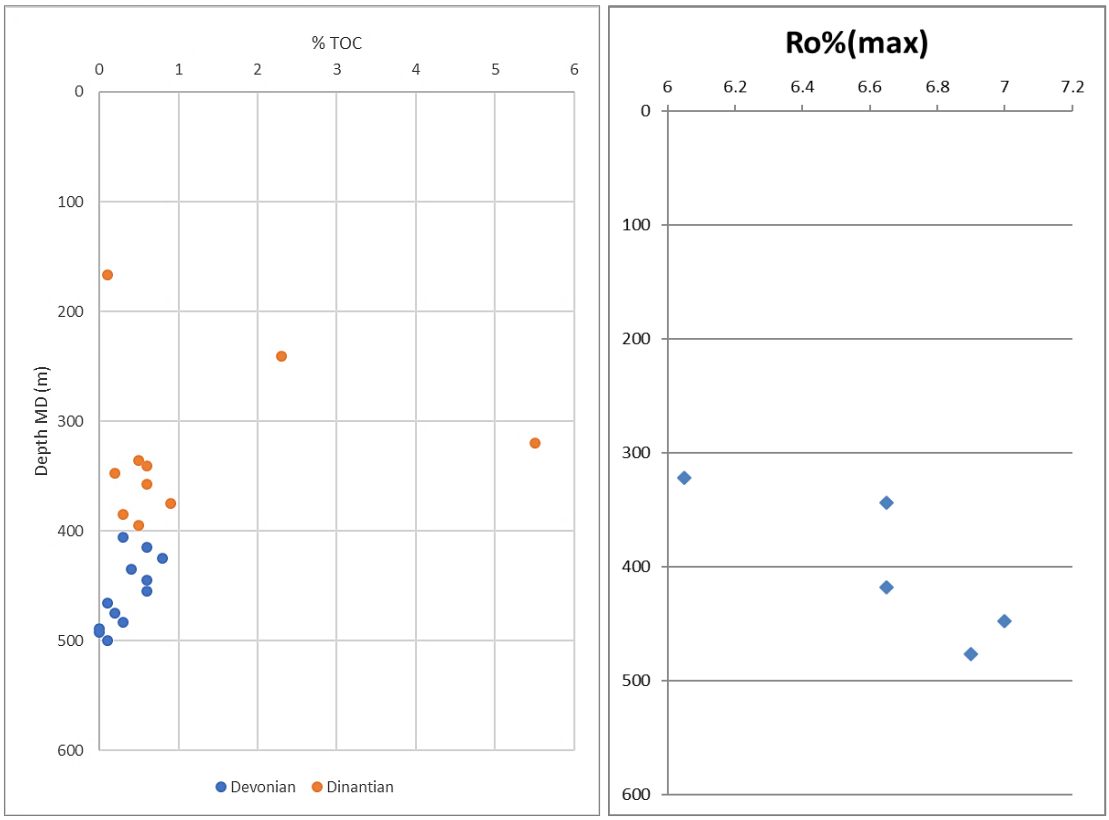

Figure 6-5: TOC content (left) and vitrinite reflectance (right) measured for the KSL-02 well samples (from Bless et al., 1981).

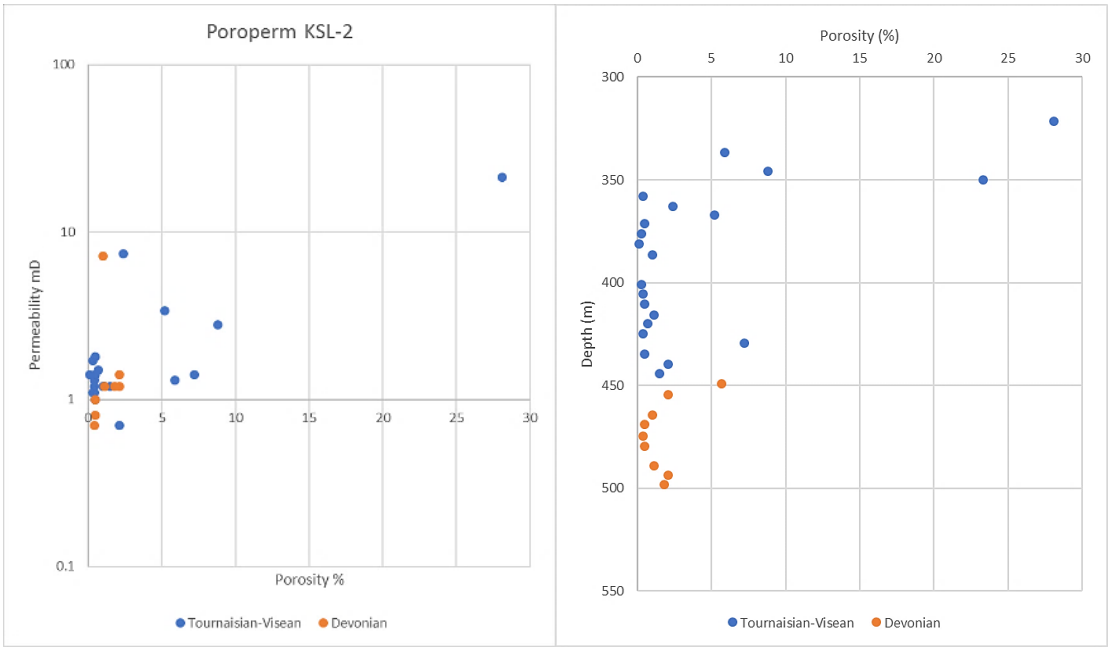

Figure 6-6: Petrophysical data of the KSL-02 well (from Bless et al., 1981).

6.3 Stratigraphy

The official stratigraphy from NLOG has been slightly modified by introducing a stratigraphic unit between the Bosscheveld Formation and the Beveland Member.

Table 6-5: Stratigraphy of the KSL-02 well, modified in respect to the NLOG website (modifications indicated by *).

Stratigraphical Unit	Top interval	Base interval
QUATER. UNDIFF.	0	7
Houthem Formation	7	17
Maastricht Formation	17	79
Gulpen Formation	79	154
Vaals Formation	154	198
Aken Formation	198	201
Schouwen Member	201	338
Beveland Member	338	382
Pont d'Arcole Formation*	382*	397*
Bosscheveld Formation*	397*	501*

6.3.1 Dinantian interval

The occurrence of more or less important faults between 201.20 and 335 m I this well cannot be excluded. Therefore, the lithological subdivision presented by Bless et al. (1981) (Table 6-6) is merely descriptive. The lithology of KSL-02 shows the upper part of the Carboniferous completely silicified (between 207.20 and 335 m). Below 335 m marine carbonates occur, also extending in the Devonian interval. This well is considered as the parastratotype of the Pont d'Arcole Formation described by Laenen, (2003), while this unit is basically not considered in the Netherlands. The well was completely described again within the framework of the SCAN project. The overview of the sedimentological log is shown in Figure 6-7. An image of higher resolution is available in Appendix B.

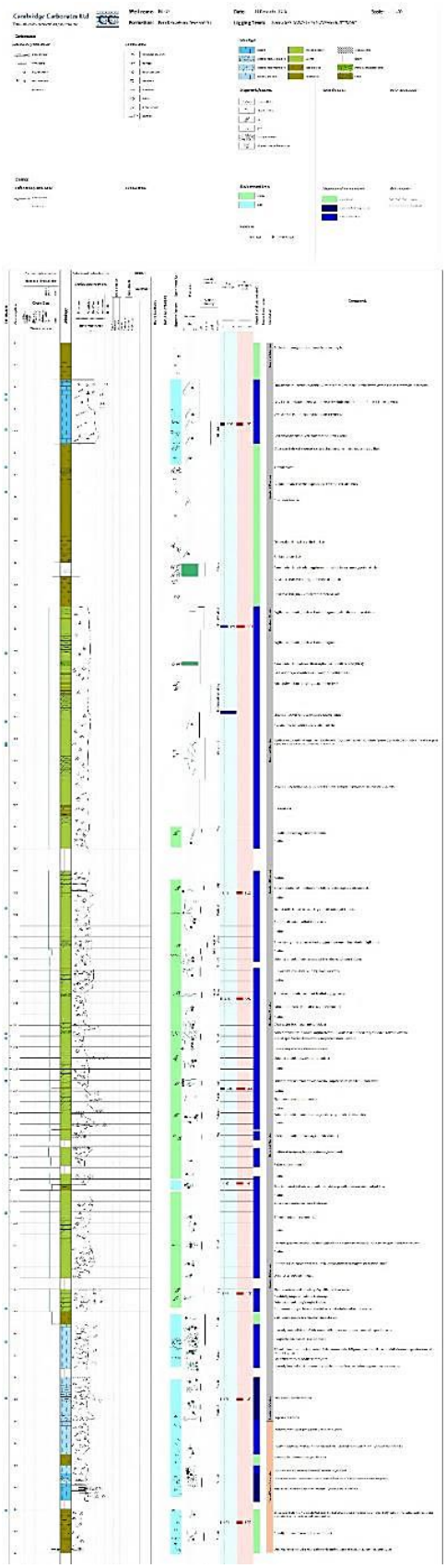

Figure 6-7: Overview of the sedimentological log constructed for KSL-02 well (an image of higher resolution is available in Appendix B).

Table 6-6: Lithological description of the KSL-02 well presented by Bless et al. (1981).

201.20 m	Top Carboniferous
201.20-335.00 m	Incompletely known sequence. Dark grey to black, silicified shales and carbonates with small geodes.
335.00-338.00 m	Light-grey limestone with bioturbations.
338.00 345.00 m	Dark-grey to black, silicified carbonates. Karst dissolution and brecciation. Geodes.
345.00-377.00 m	Dark grey to black, crinoidal dolostone, becoming argillaceous in lower part. Karst breccias and geodes. At 364 m tectonic breccia.
377.00-382.00 m	Grey to dark-grey, brecciated argillaceous limestone.
382.00-394.00 m	Dark-grey, fossiliferous pyritic mudstone with crinoid-bryozoan assemblage. Slumped and partly brecciated in lower part.
394.00-397.0A m	Dark-grey, fissile pyritic crinoidal shale. With minute-sized plant debris.
397.00-400.00 m	Dark-grey, fossiliferous calcareous mudstone.
400.00-408.00 m	Dark-grey, fossiliferous argillaceous limestone with nodular bedding. Thin karst and breccia horizons.
408.00-422.00 m	Dark-grey, fossiliferous calcareous mudstone, becoming more nodular in lower part. Strong H_2S smell.
422.00-441 .00 m	Dark-grey mudstone and nodular, calcareous mudstone, becoming more sandy below 435 m. Frequent encrinite bands.
441.00-451.50 m	Dark grey, fossiliferous sandy mudstone and nodular, calcareous mudstone. Below 447 m siltstone and sandy limestone predominate.

Although Bless et al. (1981) reported karst features in the KSL-02 core, that observation is not supported in this evaluation. Most breccias appear to have a tectonic origin. Bless et al. (1981) also reported the description of some thin sections as following:
239.80 m: Quartz grains of silt size (0.2-0.4 mm Ø), some feldspar, pyrite grains, some illite-sericite flakes and some dolomite (the latter normally as idiomorphic rhombs) occur in a carbonaceous groundmass. This rock grades into a poorly carbonaceous, clayey siltstone with intergranular kaolinite-aggregates and sericite-illite flakes.
349.45 m: Carbonaceous, dolosparite with isolated quartz grains of silt size and pyrite grains. Narrow veins are filled with dolomite crystals.
427.95 m: Carbonaceous, silty biomicrite with calcitic fossil fragments and lumps. Silt-sized quartz grains and feldspar, some sericite and chlorite. Abundance of small pyrite particles (0.01-0.02 mm Ø). Lumps partly rectangular, the latter may be up to 2 mm Ø.

6.4 Depositional environment

The depositional environment is mostly basinal, characterised by a proximal basin followed by a rapid deepening during late Warnantian (Brigantian).

6.5 Biostratigraphy

Bless et al. (1981) presented a biostratigraphic framework based on the micropalaeontological data and correlations with nearby wells (Table 6-7):

Table 6-7: Biostratigraphic framework based on Bless et al. (1981) and modifications applied during SCAN projects.

Interval (m)	Bless et al. (1981)	Comments	Revised Age
207.20-280	attributed to the V1/V2. This age is based on foraminifers at 206 m in this hole and at 250-260 m and 270-280 m in the nearby KSL-01.	In this interval Bless et al. (1981) document *Endothyra*, that is not biostratigraphically useful (found also in V3c of S02-2 and in Waulsortian reefs, V1). *Plectogyranopsis* cf. is typical of Upper Tournaisian-Upper Visean Interval. In Kastanjelaan-1 (DB123), the only diagnostic foraminifer is an uncertain form, cf. *Tournayellina pentacamerata*, of Tournaisian age (could be a reworked form). Gamma-ray correlation with other wells points to a Visean age for this interval, up to V3c	Generic Visean
280-335	No biostratigraphic control		No biostratigraphic control
335-400	The top of the interval is dated as Tn2b-c by means of conodonts and corals. The base of this interval is dated asTn2a by means of corals. The spore assemblage in this lower part suggests a Tn1b to Tn2 age, whereas the ostracods suggest rather a Tn1b age. The lithology of this basal part (shales and mudstones) strongly resembles that of the Tn2a Pont d'Arcole shales in Belgium. Therefore, we attribute the complete 335-400 m sequence to the Tn2.	Some of the considerations are based on wrong ages, as the Pont d'Arcole Fm is normally Tn1b. Therefore, the interval should be expanded towards a broader Tn1b-Tn2. The corals (*Siphonophyllia* sp., *Cyathaxonia cornu*) found at 380.55 m and described by Bless at al. (1981) are also compatible with an upper Tn1b age: we could suppose that this could be the boundary between the Tn1b and Tn2a intervals. At 335-337, the presence of the coral *Saleelasma delepini* point to an age Uppermost Tn1, Tn2.	400-380 Tn1b 380-335 Tn2
400-445	This interval is here attributed to the Tn1b. This age is based on a mixture of partly conflicting arguments. The ostracods in the entire interval suggest a Tn1b age. The foraminifers point to a Tn1b age except for the possibly phylogenetic evolution of the genus *Earlandia* that suggests a T2b age for the 400-408 m interval. The corals seem characteristic of the Tn1b, although some		Tn1b

	Strunian (Fa2d + T1a) elements have been found between 436 and 445 m. Brachiopods at 438 m strongly resemble Strunian forms.		
445 and 462	all fossils (spores, foraminifers, ostracods, corals and brachiopods) point to a Strunian age. Between 465 and 470 m, the spores suggest an Upper Famennian (Fa2c) age, which fits well with the ostracod assemblage in this interval.		Devonian
Below 470	no biostratigraphic control is available. This sequence (470-500.10 m) is arbitrarily attributed to the Upper Famennian.		

6.6 Sequence stratigraphy

Ten depositional cycles have been recognised in the Dinantian succession of KSL-02 that have been grouped as follows according to the gamma-ray character (Table 6-8).

Table 6-8: Sequence stratigraphic scheme used on KSL-02 well.

Depositional cycles	Gamma ray character	Depositional setting
3b	Gamma ray increases upwards to very high followed by low gamma ray HST	Condensed deposition in basin during LST and TST; high stand shedding of carbonates into basin.
3a		
2d	Generally high gamma ray.	Distal carbonate ramp or basin.
2c		
2b		
2a		
1d	Moderate to low with moderate to high peaks interpreted as max. flooding followed by low gamma ray HST	Distal carbonate ramp with increasing carbonate input as ramp progrades during in HST. Maximum flooding events marked by high gamma intervals.
1c		
1b	Very high gamma ray with low gamma ray top	Establishment of deep water in basin followed by Dolomitised deep ramp carbonates.
1a	Low to moderate gamma ray HST	Initial transgression of basin.

The overall depositional setting of the KSL-02 well is interpreted as basinal in which the carbonate intervals were introduced in the form of redeposited platform sediment. The depositional cycles are interpreted in terms of the evolution of surrounding carbonate platforms.

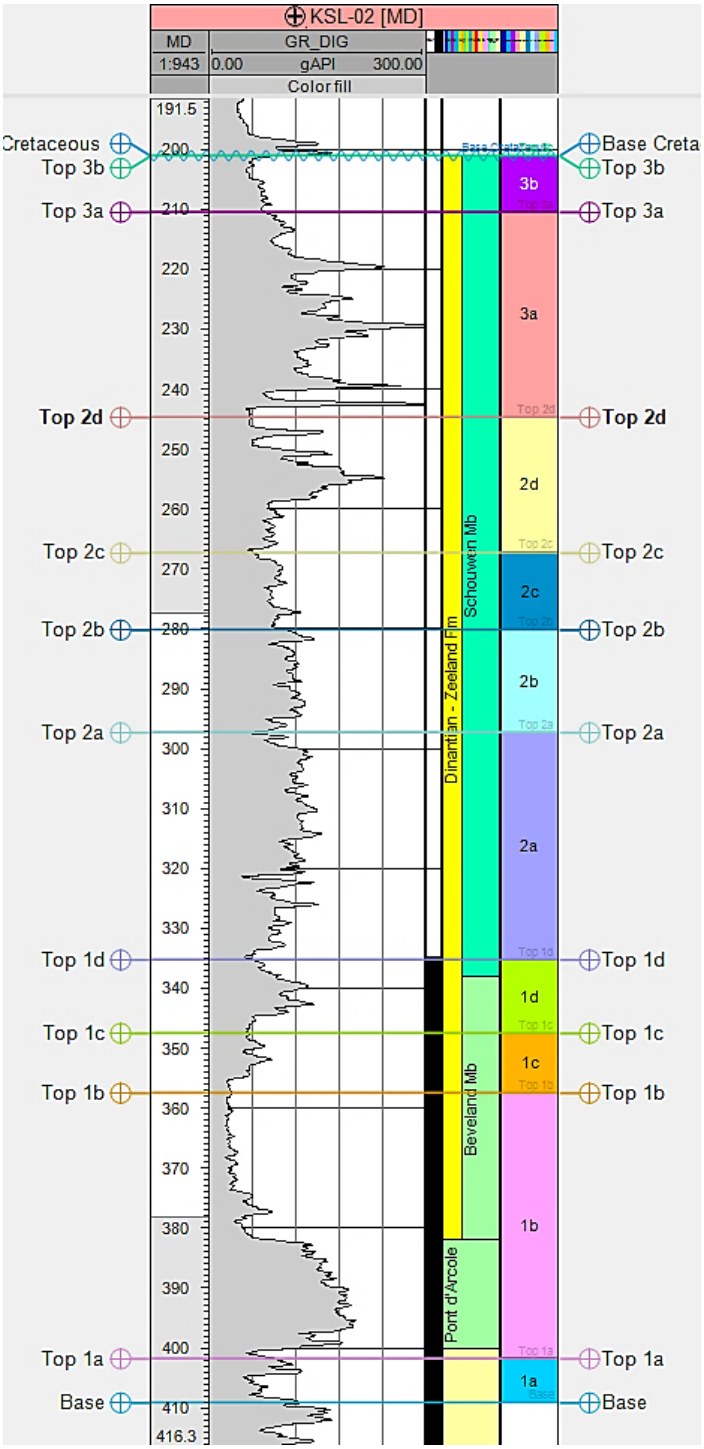

Figure 6-8: Depositional cycles recognised in the KSL-02 well.

1a and 1b depositional cycles: These cycles are interpreted as the initial deposits of the basin following the late Tournaisian/early Visean transgression. The 1a depositional cycle is interpreted as shallow water carbonates deposited during the initial transgression of basin. Core in KSL-02 shows that the high gamma-ray interval of the 1b depositional cycle, equivalent to the Pont d'Arcole Formation, represents deep water argillaceous limestone and shale. The upper, low gamma-ray part of the 1b cycle consists of dolomitised wackestone and carbonate mudstone deposited in a basinal or deep ramp setting.

1c and 1d depositional cycles: The 1c depositional cycle is cored in KSL-02 and consists of dolomitised bioclastic wackestone and carbonate mudstone deposited in a are interpreted as distal carbonate ramp facies; the initial low gamma-ray signature reflects the deposition of redeposited carbonates sourced from shallow to mid-ramp settings during the TST. The higher gamma-ray interval represents the drowning of the source of redeposited carbonates during the maximum flood. The high at the top of the cycle is interpreted as increased supply of redeposited carbonates as the carbonate ramp progrades during the HST. The 1d depositional cycle consists of deep water argillaceous limestone and shale.
2a to 2c depositional cycles: These cycles have a higher, more uniform gamma-ray signature, they are interpreted as distal ramp or carbonate slope facies, possibly associated with a transition from carbonate ramp- to flat-topped carbonate platform in surrounding area. The low gamma-ray intervals interpreted as influx of resedimented carbonates during high stands. The overall high gamma-ray signature in KSL-02 suggests that this was deposited in a distal basinal setting.
2d to 3b depositional cycles: These cycles show an increasing-upward gamma-ray signature that are interpreted as distal carbonate slope or basinal facies. The high gamma-ray intervals are interpreted LST to TST intervals when there was no carbonate production on platforms on exposed carbonate platforms and no export of peri-platform carbonates to the surrounding basin. The low gamma-ray intervals are interpreted as HSTs when carbonate production was taking place on flooded carbonate platforms with some high stand shedding of carbonates to the basin.

6.7 Microfacies

The available thin sections of the TNO collection are from the Bosscheveld and Zeeland Formations. Different microfacies were observed in the different formations and their members.

6.7.1 Bosscheveld Formation

A total number of 23 thin sections of the Bosscheveld Formation were studied. The Bosscheveld Formation consists of siliciclastics and carbonates. The transition from siliciclastics is most likely gradual (Figures 6-9 and 6-10).

6.7.2 Pont d'Arcole Formation

The facies of the Pont d'Arcole Formation (Figure 6-11) are similar to that of the Bosscheveld Formation. Depending on the lithostratigraphic scheme used the Pont d’Arcole is sometimes considered part of the Bosscheveld Formation.

6.7.3 Beveland Member (Zeeland Formation)

In the Beveland Member siliciclastic grains are rare. The Beveland Member consists mostly of dolomite. The precursor limestone facies is inferred to be bioclastic wacke- and packstone (Figure 6-12).

6.7.4 Schouwen Member (Zeeland Formation)

Only three thin sections of the Schouwen Member exist. These consist of bioclastic wacke- to grainstone (Figure 6-13).

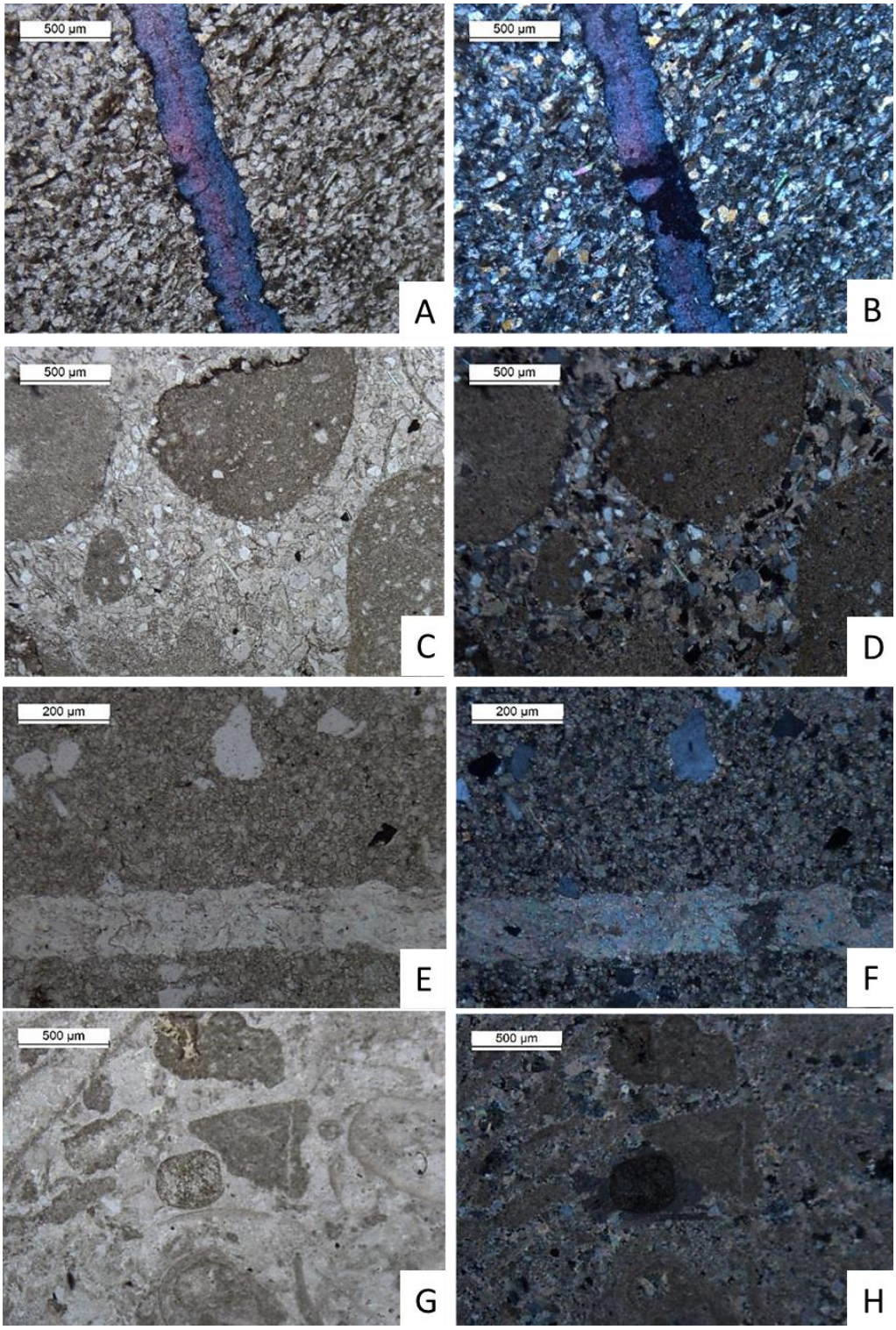

Figure 6-9: Representative photomicrographs (PPL and corresponding XPL) of the facies types observed in Bosscheveld Formation encountered in the KSL-02 well. A, B) Sandstone with ferroan calcite vein (498.75 m). C, D) Sandstone with carbonate intraclasts (492.95 m). E, F) Dolomitised silty mudstone with angular quartz grains (476.75 m). G, H) Bio- intraclastic grainstone (462.20 m).

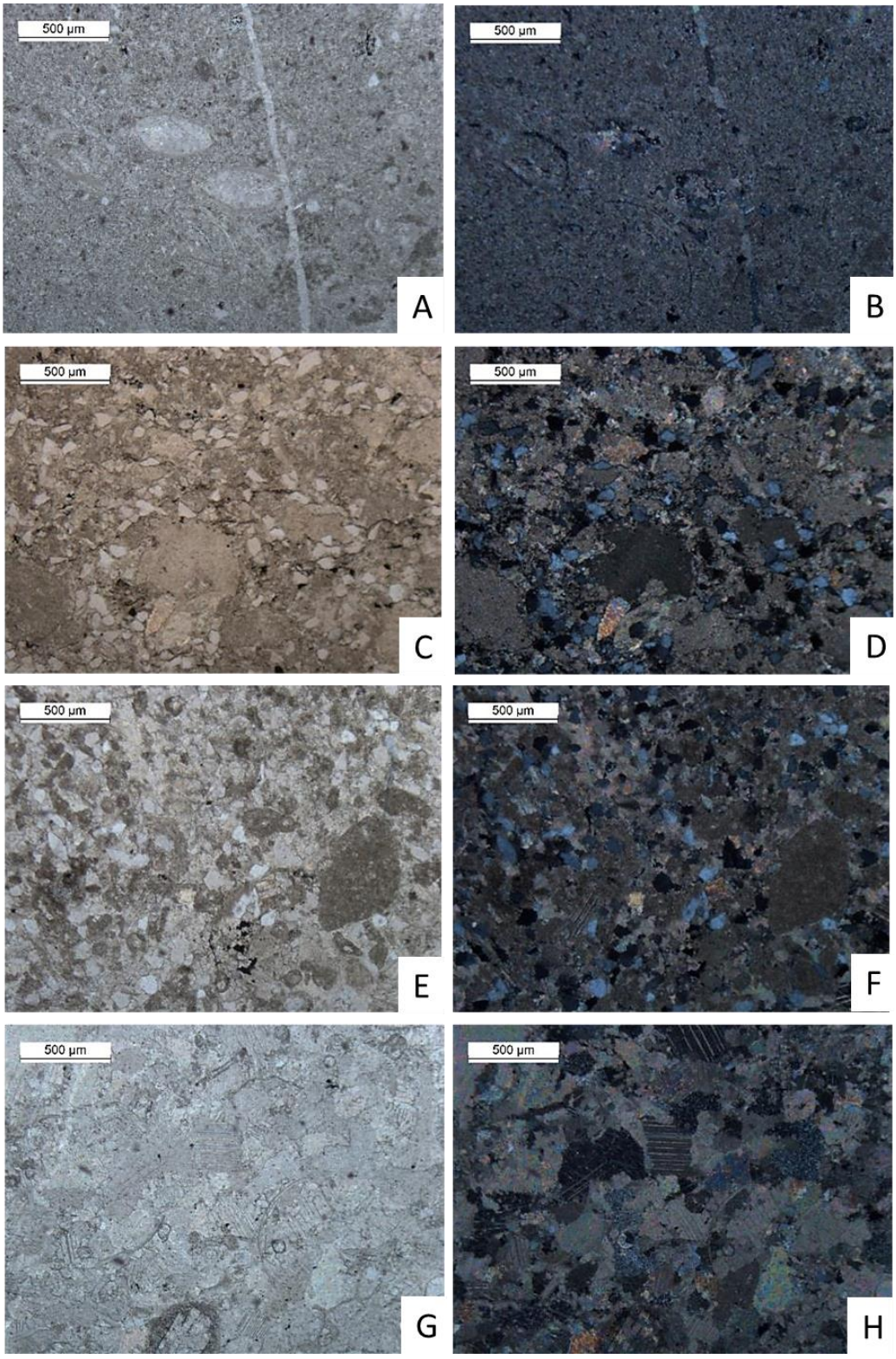

Figure 6-10: Representative photomicrographs (PPL and corresponding XPL) of the facies types observed in Bosscheveld Formation encountered in the KSL-02 well. A, B) Bioclastic wackestone (462.20 m). C, D) Silty crinoidal wacke-packstone (452.70 m). E, F) Silty micritic grain/intraclast grainstone (451.10 m). G, H) Bio-intraclastic grainstone (429.10 m).

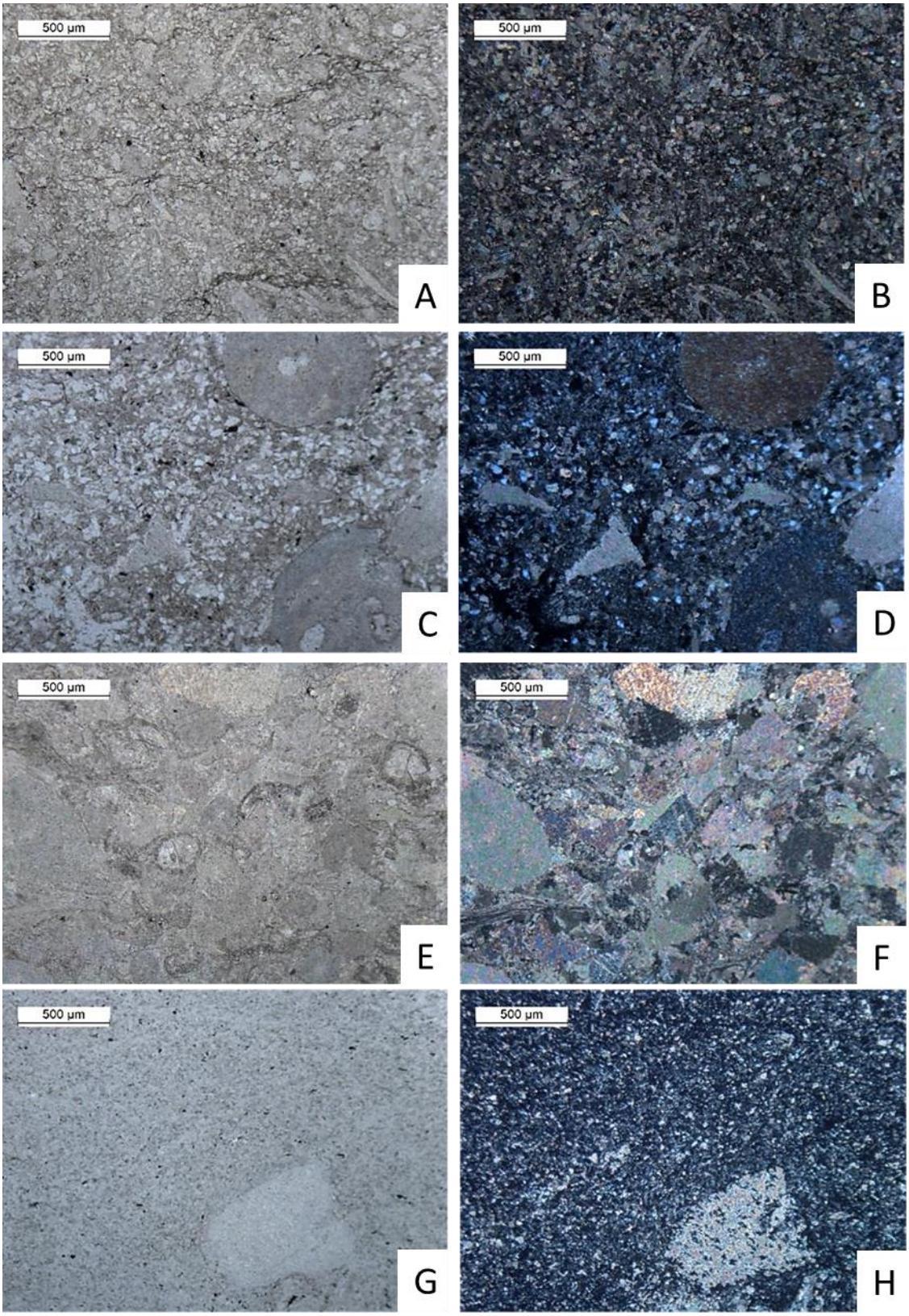

Figure 6-11: Representative photomicrographs (PPL and corresponding XPL) of the facies types observed in the Pont d'Arcole Formation encountered in the KSL-02 well. A, B) Dolomitised bioclastic packstone (397.40 m). C, D) Silty crinoidal wackestone (396.60 m). E, F) Bioclastic/crinoidal pack-grainstone (391.80 m). G, H) Silicified mudstone (386.05 m).

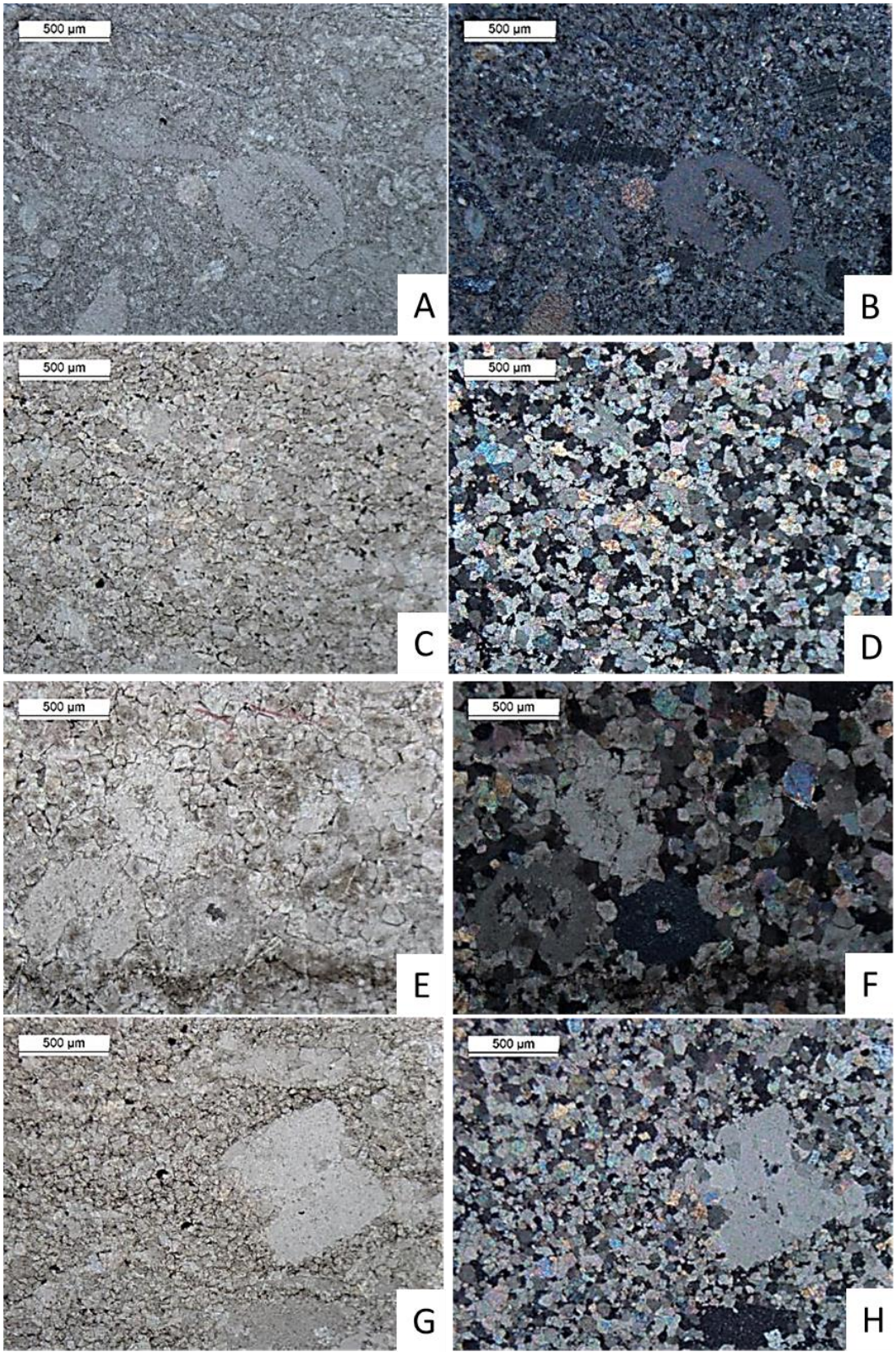

Figure 6-12: Representative photomicrographs (PPL and corresponding XPL) of the facies types observed in the Beveland Member encountered in the KSL-02 well. A, B) Bioclastic packstone (380.95 m). C, D) Dolomitised bioclastic wackestone (366.20 m). E, F, F, G) Dolomitised bioclastic wackestone (351.30 m).

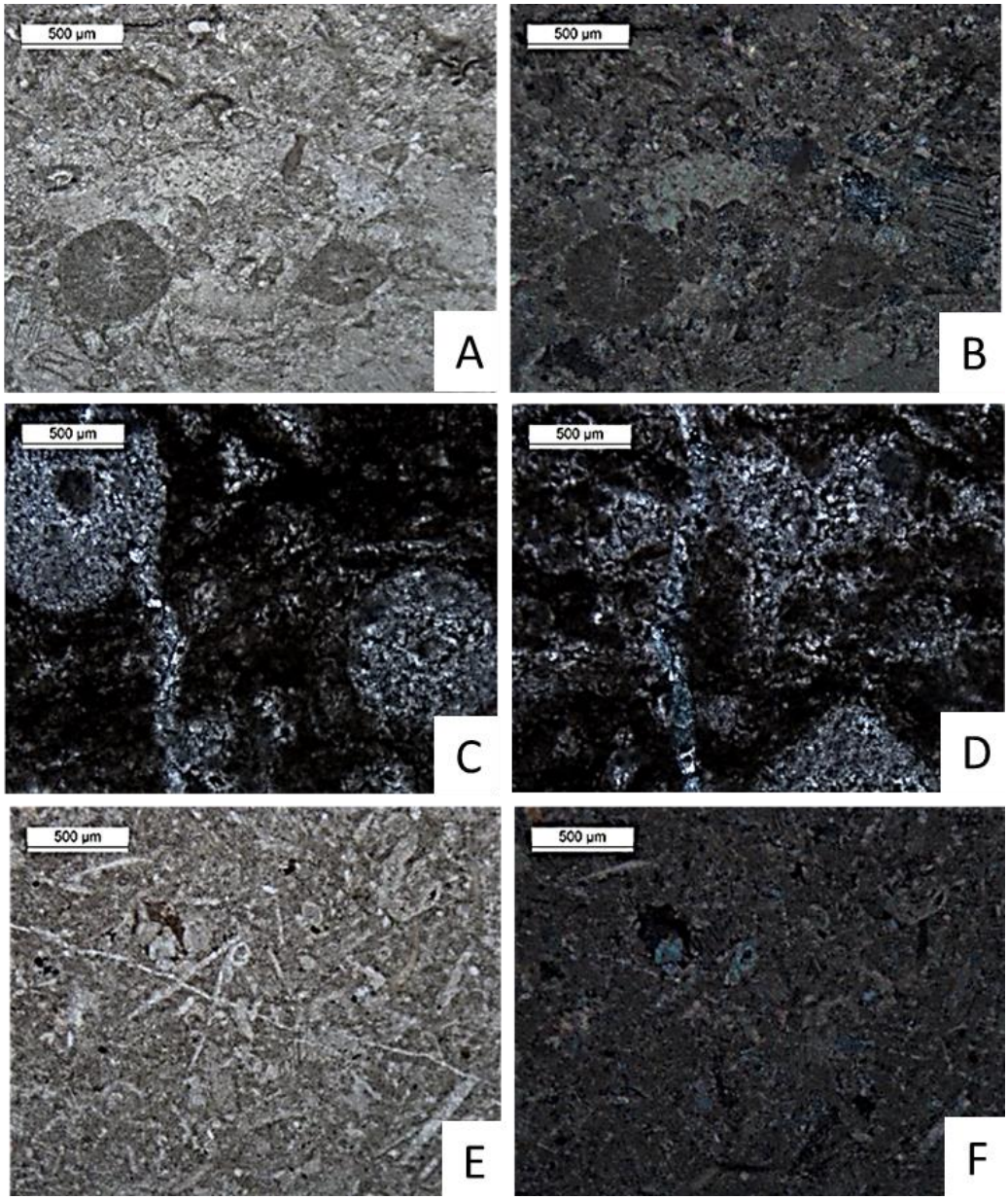

Figure 6-13: Representative photomicrographs (PPL and corresponding XPL) of the facies types observed in the Schouwen Member encountered in the KSL-02 well. A, B) Crinoidal grainstone (336.95 m). C, D) Dolomitised bioclastic mud-wackestone (335.60 m). E, F) Bioclastic packstone (335.55 m).

6.8 Diagenesis

6.8.1 Petrographic observations and paragenetic sequence

A paragenetic sequence was established for the KSL-02 based on the study of existing thin sections (n = 44) of the TNO collection. The thin sections are from the Bosscheveld Formation (n = 23) and the Pont d'Arcole Member (n = 4), Beveland Member (n = 14) and Schouwen Member (n = 3) of the Zeeland Formation.
The paragenetic sequence identified in this well is:

1. Early calcite cementation: C1 + C2 (+syntaxial calcite), possibly locally ferroan
2. Chemical compaction: Chemical compaction commenced before and after pervasive dolomitisation.
3. Pervasive dolomitisation and saddle dolomite veins: This phase post-dates chemical compaction.
4. Calcite veins cemented by equant calcite
5. Silicification
6. Recrystallisation

Note that in the KSL-02 dolomite occurs mostly in the upper part of the core (i.e. 347.1 m - 372.55 m) in the Beveland Member which is not cored in the HEU-01-S1. The link between the diagenetic phases of the KSL-02, HEU-01-S1 and GVK-01 is given in Figure 6-14. The different diagenetic phases are illustrated in Figures 6-15 and 6-16.

HEU-01	KSL-02	GVK	Diagenetic phase
+	+	A?	C1
+	-	MD?	D1
+	+	B?	C2
+	+	+	Stylolites
+	+	-	D2
+	+	-	C3
+	+	+	Si
+	+	-	Recrystallisation

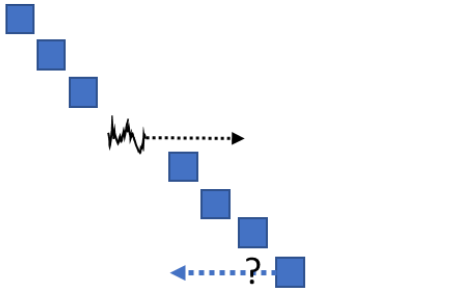

Figure 6-14: Overview of the diagenetic phases and their presence in the HEU-01-S1, KSL-02 and GVK-01. A, MD and B are cement phases described by Mathes-Schmidt (2000) for the GVK-01 well. Cement A and syntaxial calcite = C1; Matrix dolomite MD = D1 (The dolomite crystal habit is described as subhedral and no mention of saddle dolomite cement is made, therefore the dolomite is interpreted as an early matrix dolomite); Blocky calcite cement B = C2.

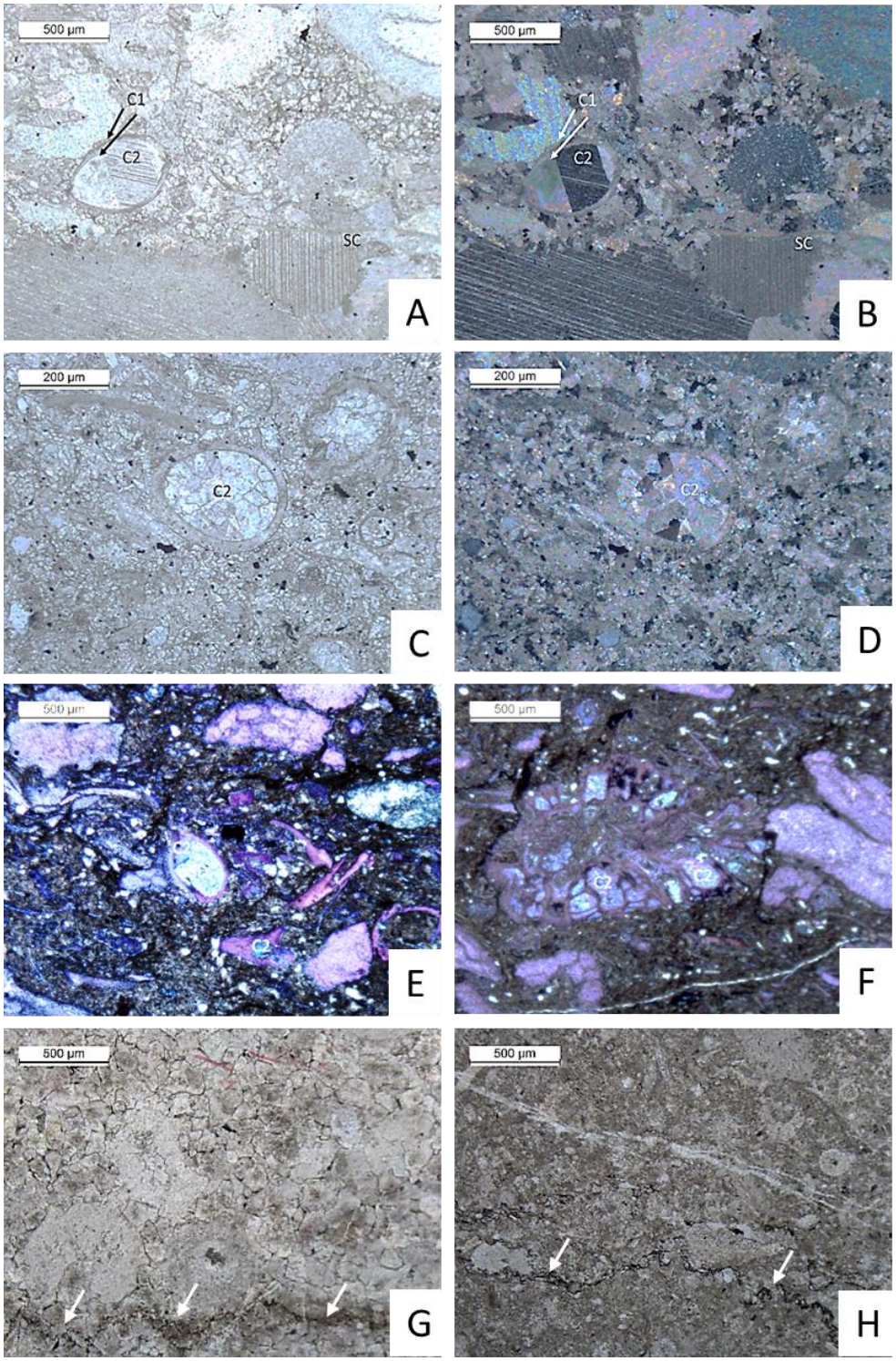

Figure 6-15: Representative photomicrographs of the diagenetic phases observed in the KSL-02 well. A, B) PPL and corresponding XPL image of calcite cements, C1 - fine columnar calcite fringing components, C2 - fine to coarse crystalline equant calcite cementing pore space (429 m). C, D) PPL and corresponding XPL image of calcite cements, C2 - equant calcite cementing pore space (425.90 m). E, F) PPL image of stained thin sections showing C2 – In silty shales and mudstones. The C2 calcite is ferroan. Note the presence of non-ferroan saddle dolomite (SD) (427.95 m). PPL image showing chemical compaction pre- and post-dating the pervasive dolomitization (arrows): G) Smeared stylolite, partially incorporated in the dolomite crystals (stylolite pre-dates dolomitisation) (351.30 m). H) Sharp stylolite cross cutting dolomitised bioclastic packstone (stylolite post-dates dolomitisation).

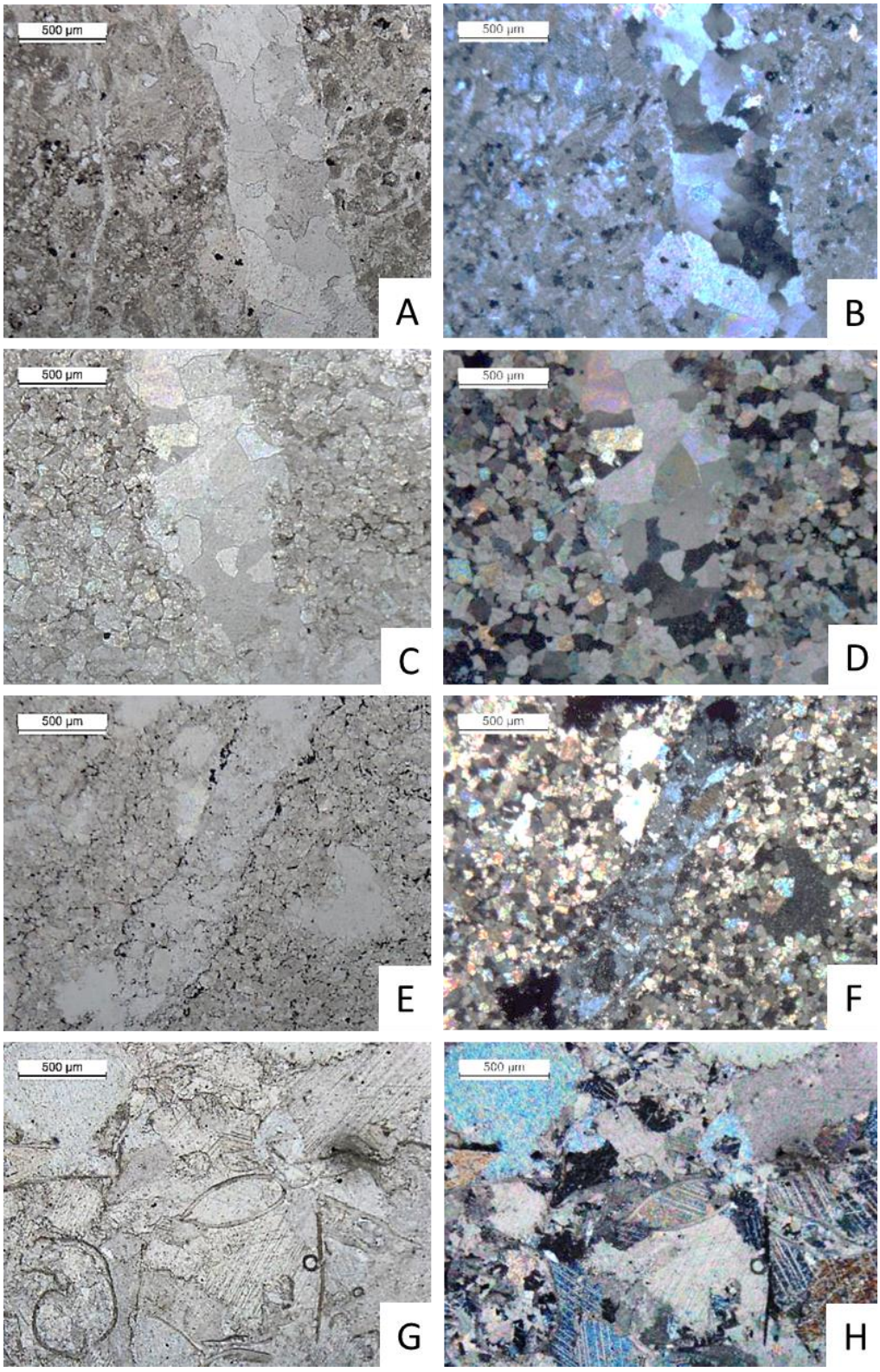

Figure 6-16: Representative photomicrographs (PPL and corresponding XPL) of the diagenetic phases observed in the KSL-02 well. A, B) D2: Saddle dolomite veins cross cut limestone host rock (422 m). C, D) C3: Calcite vein post-dating dolomitisation (369.9 m). E, F) SI: Silicification post-dates dolomitisation and C3 calcite (364.6 m). G, H) Recrystallisation – poikilotopic calcite and crystal twinning (435.25 m).

6.8.2 Cathodoluminescence

Of the samples selected for further diagenetic analysis three samples consist of dolomite, i.e. 351.20 m, 364.40 m and 366.55 m, and two samples consist of coarse crystalline calcite, i.e. 338.65 m and 378.40 m. The dolomite samples are representative for the D2 dolomite. The calcite samples are representative for the C3 calcite cement.

D2: The matrix of the dolomite is fine crystalline and consists of sub- to anhedral crystals. The dolomite cement lining veins consists coarser and is characterised by saddle dolomite crystals. The transition from dolomite matrix to vein can be gradual (Figure 6-17 A and B). The both the dolomite matrix and cement is generally dull luminescent. A bright luminescent zone can be observed in the saddle dolomite (Figure 6-17 C and D). The rim of the saddle dolomite crystals is non-luminescent, and a minor phase of dissolution may pre-date the precipitation of the non-luminescent dolomite (Figure 6-17 E and F).

C3: The C3 calcite is coarse crystalline and twinned. It is characterised by fairly wide, dull to non- luminescent bands (Figure 6-18 A to D).

Si: Quartz cement precipitation or silicification of the pre-dating diagenetic phases or host rock post-dates the D2 dolomite and C3 cement. Locally the quartz cement is associated to a phase of fracturing and brecciation. The quartz can be both crystalline and amorphous (Figure 6-18 E to G).

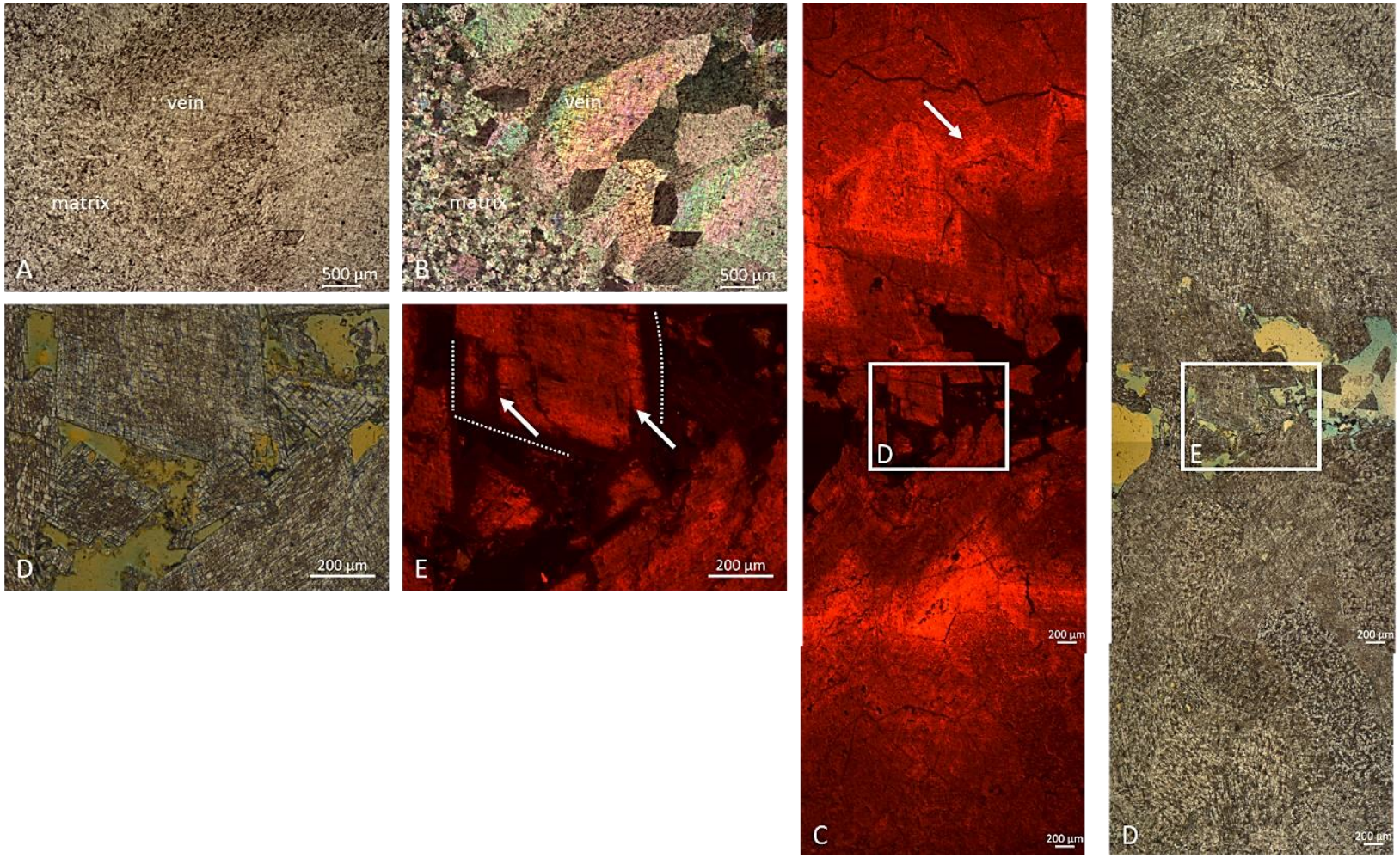

Figure 6-17: A, B). Equivalent plane and cross polarised light microphotographs. Fine crystalline matrix dolomite consisting of sub- to anhedral fine crystals gradually change to coarse, crystalline saddle dolomite (366.55 m). C to F) Equivalent plane polarised and cathodoluminescence microphotographs. Saddle dolomite cemented vein consisting mostly of dull luminescent dolomite with occasional bright luminescence zones (white arrow, C). A final phase of non-luminescent dolomite occurs in the centre of the vein. A phase of corrosion/dissolution (see white arrow, F) may pre-date the non-luminescent dolomite (366.55 m).

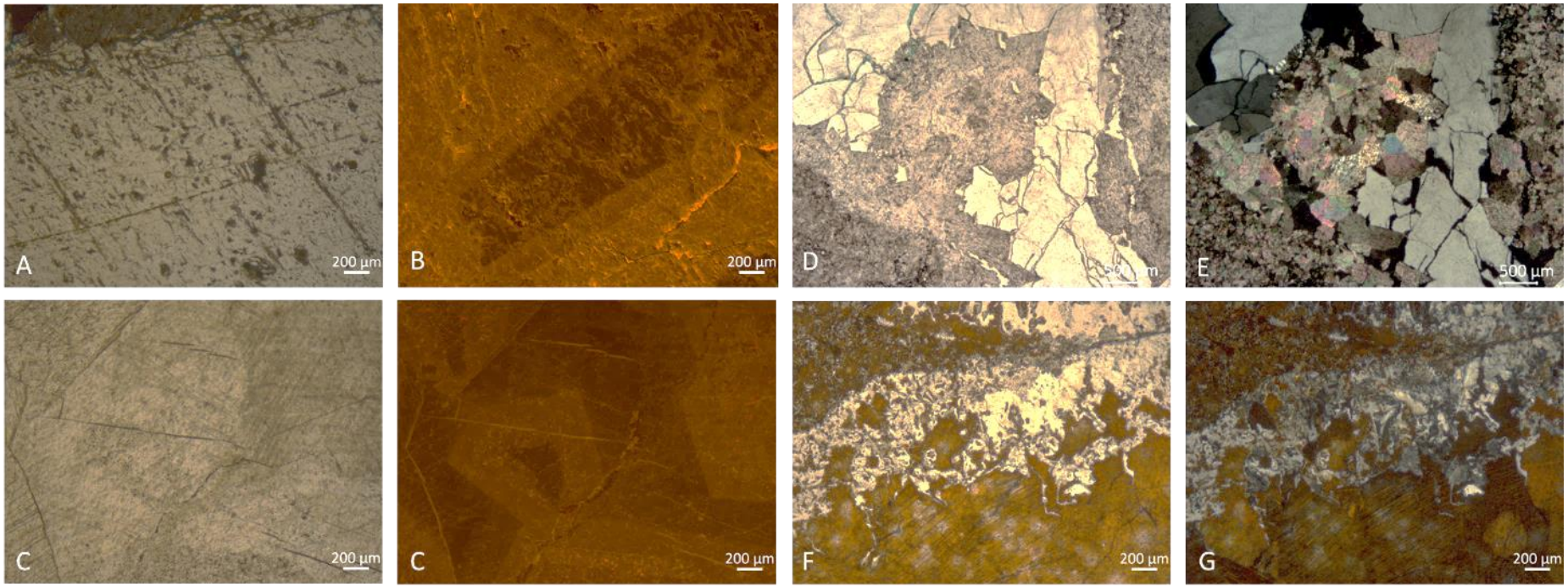

Figure 6-18: A, B) Equivalent plane polarised and cathodoluminescence microphotographs. Coarse crystalline calcite C3 with dull and non-luminescent zones (338.65 m). C, D) Coarse crystalline calcite C3 with dull and non-luminescent zones (378.40 m). D, E) Equivalent plane and cross polarised microphotograph. D2 dolomite post-dated by quartz cement (351.10 m). F, G) Equivalent plane and cross polarised microphotograph (stained thin section). Silicification of the C3 calcite. The silica is amorphous.

6.8.3 Stable isotope results

The stable isotope results of the samples selected from the KSL-02 core are given in Figure 6-19 and Table 6-9. The selected samples (n = 7) originate from the samples selected for CL. Compared to the marine reference value the stable isotope signature of the KSL-02 host rock/matrix is depleted. Only one data point of the KSL-02 matrix is available. It falls well within the range of other matrix signatures of the BHG-01, O18-01, S05-01 and KTG-01. The dolomite vein samples are characterised by more depleted $\delta^{18}O$ values than the equivalent matrix. Calcite cements occurring in veins are characterised by deleted $\delta^{18}O$ values and $\delta^{13}C$ values.

In the KSL-02, HEU-01-S1 and GVK-01, no evidence of karst processes have been observed, while the occurrence of coarse crystalline, saddle dolomites are evidence of high temperature events. Therefore the resetting of the KSL-02 matrix signature is interpreted as the result of recrystallisation due to high temperature diagenetic processes. The depleted $\delta^{18}O$ values and $\delta^{13}C$ values of the calcite cement occurring in veins suggests the calcite veins precipitated from a high temperature fluid. A late calcite cement is almost always precipitating following high temperature dolomitisation. This calcite cement is also interpreted as a calcite phase associated with and post-dating high temperature dolomites.

Table 6-9: Stable isotope results of the KSL-02 samples expressed in per mill VPDB.

Sample (m)	Mineralogy	phase	$\delta^{13}C$	$\delta^{18}O$
338.65	Calcite	Vein	0.7	-9.6
378.4	Calcite	Matrix	1.9	-6.6
351.2	Dolomite	Matrix	1.7	-5.1
366.55	Dolomite	Matrix	1.7	-6.5
378.4	Calcite	Vein	-0.7	-10.0
351.2	Dolomite	Vein	1.5	-7.2
366.55	Dolomite	Vein	1.1	-9.1

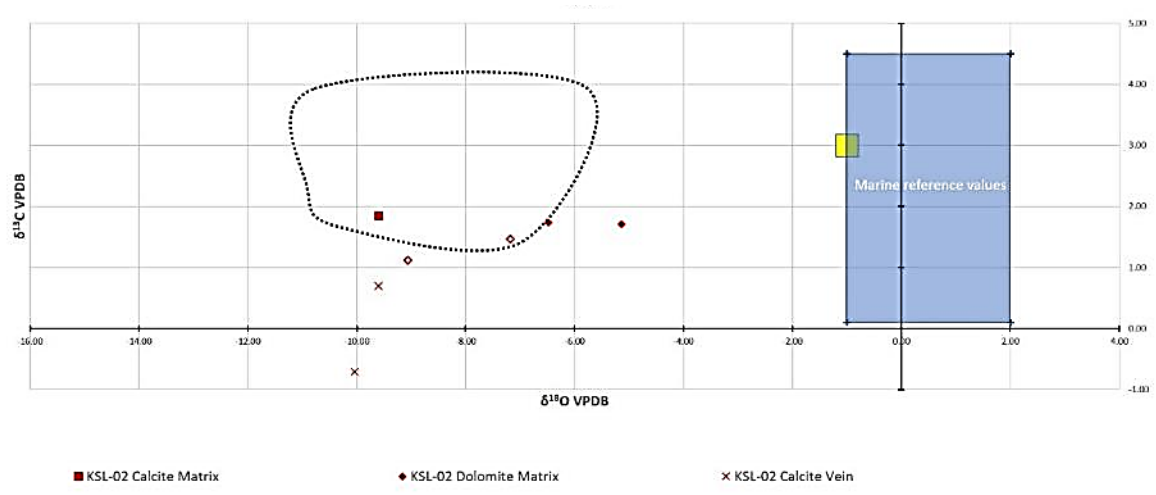

Figure 6-19: Stable isotope cross plot of the KSL-02 samples. The dotted line represents the limestone host rock/matrix signature obtained from the other studied wells with the exception of UHM-01. The reference values of Dinantian marine limestones; yellow area after Muchez et al. (1991) and blue area after Nielsen (1994).

6.8.4 Fluid inclusion microthermometry

D2/366.55 m: Fluid inclusion microthermometry of the D2 dolomite shows that it precipitated from a high temperature fluid: 105.1 - 176.3 °C, average 125.1 °C (Figure 6-20, Table 6-10). The salinity of the fluid covers a wide range. Most Tm ice measurements indicate salinities of 0 - 10.1 wt. % eq. NaCl (Figure 6-20). One measurement indicates extremely high salinity of 27.7 wt. % eq. NaCl. Mixing of a high and a low salinity fluid may have occurred.

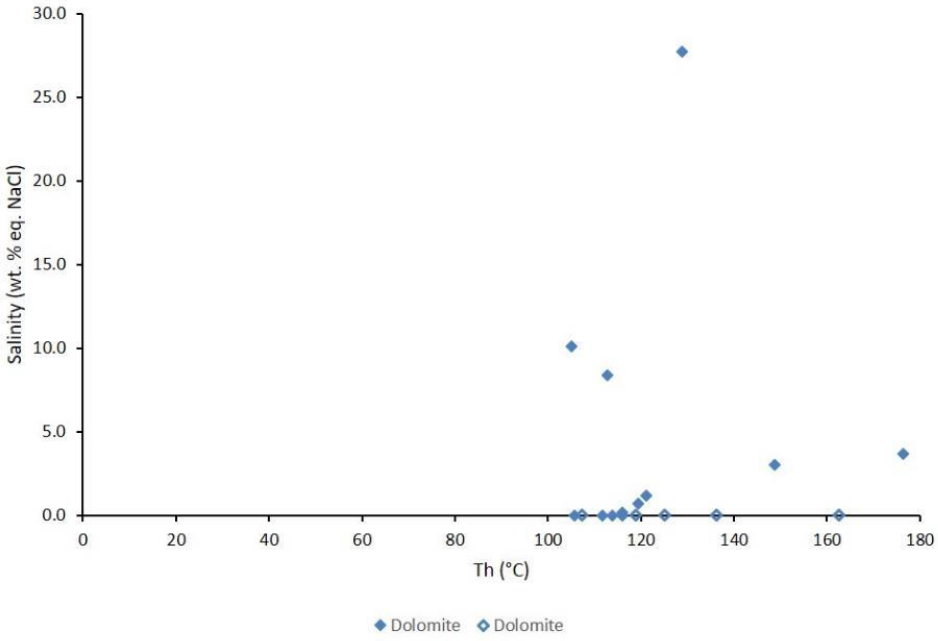

Figure 6-20: Temperature salinity cross plot of the D2 dolomite (KSL-02 366.55 m). Inclusions for which Tm ice could not be observed have been were attributed an arbitrary salinity of 0 wt. % eq. NaCl. These data points are marked by symbols without fill.

Table 6-10: Overview of the microthermometry results of (KSL-02 366.55 m D2). N.o. = not observed.

F. i. Number	F. i. Type	F. i. Host mineral	F. i. Host type	$T_{m\,ice}$ (°C)	Salinity (wt. % $NaCl_{eq}$)	T_h (°C)
1	aq	dolomite	primary	0.0	0.0	116.0
2	aq	dolomite	primary	0.0	0.0	113.8
3	aq	dolomite	primary	0.0	0.0	105.8
4	aq	dolomite	primary	0.0	0.0	111.8
5	aq	dolomite	primary	-0.4	0.7	119.4
6	aq	dolomite	primary	-0.1	0.2	116.0
7	aq	dolomite	primary	-0.7	1.2	121.1
8	aq	dolomite	primary	n.o.		125.1
9	aq	dolomite	primary	*-28.7*	*27.7*	128.9
10	aq	dolomite	primary	n.o.		162.6
11	aq	dolomite	primary	-2.2	3.7	176.3
12	aq	dolomite	primary	-5.4	8.4	112.8
13	aq	dolomite	primary	-6.7	10.1	105.1
14	aq	dolomite	primary	n.o.		118.8
15	aq	dolomite	primary	n.o.		107.3
16	aq	dolomite	primary	n.o.		136.3
17	aq	dolomite	primary	-1.8	3.0	148.8

6.8.5 Diagenetic sequence in the context of burial/thermal history

The elevated degree of maturity could be explained with relatively deep burial and the probable presence of an intrusive body in the region of Maastricht, documented by an important magnetic anomaly.
It is not possible to derive a burial history curve as it is impossible to model due to limitations of the easyRo algorithm. The resulting %Ro from different models never exceeds 4.68%, increasing heat flow and/or burial.

6.9 General observations

The KSL-02 was deposited in a basin, sometimes anoxic, showing a succession ranging from Famennian until Middle Visean. Apparently the thickness of the Upper Tournaisian and the Lower Visean is quite reduced or even this interval is missing: based on the available data it is not possible to confirm one scenario or the other. Extensive silicification is present in the upper part of the Lower Carboniferous sequence, probably related to the very long exposure and erosion associated with the Cretaceous unconformity.

6.10 Reservoir quality

Reservoir quality in the KSL-02 well is better than other Dinantian wells, mostly due to the effects of silicification, with porosity values up to 30% (Figure 6-21).

Figure 6-21: At 348.30 m, some vuggy, very porous, intervals are present.

Additional data from publications

Table 6-11: Vitrinite reflectance data for the KSL-02 well (Bless et al., 1981).

Depth (m)	Age	%Rmax	Samples	Remarks
319.10-321.60 ?		6.05	7	Silty claystone with abundant pyrite. Rich in inertodetrinite. Rare vitrinite. One possible Tasmanales
343.85-344.00	Tn2	6.65	2	Claystone with abundant inertodetrinite and corpocollinite(?).
417.90	Tn1b	6.65	7	Pyritic claystone with abundant inertodetrinite. Vitrinites usually too thin and small for measurements
448.25	Strunian	7.0		Siltstone with abundant inertodetrinite (Rmax 5%) and two oxidised graphite.
477.40	Famennian	6.9		Carbonate and pyritic siltstone with abundant inertodetrinite

Table 6-12: Total and organic carbon content in the KSL-02 well (from Bless et al., 1981).

Depth (m)	Ctot %	Corg %
239.80-242.00	2.3	2.3
319.70-321.60	5.8	5.5
335.80	10.9	0.5
340.60	6.5	0.6
347.20	12.0	0.2
357.20	11.3	0.6
167.00	11.9	0.1
375.00	11.2	0.9
385.00	1.7	0.3
395.00	1.8	0.5
406.00	6.7	0.3
415.00	8.7	0.6
425.10	4.5	0.8
434.50	11.2	0.4
445.00	7.9	0.6
454.50	8.4	0.6
465.25	8.1	0.1
475.00	9.5	0.2
483.10	10.0	0.3
488.90	0.9	0
492.50	2.2	0
500.00	1.9	0.1

Table 6-13: Petrophysical measurements on KSL-02 cores.

Depth (m)	Porosity (%)	Permeability (md)	Matrix density (g/cm3)
321.6	28.1	21.2	2.513
336.7	5.9	1.3	2.692
345.9	8.8	2.8	2.824
349.8	23.3		2.877
358.0	0.4	1.2	2.836
362.8	2.4	7.4	2.812
366.9	5.2	3.4	2.835
371.2	0.5	1.4	2.815
376.2	0.3	1.7	2.804
381.0	0.1	1.4	2.726
386.6	1.0	1.2	2.982
400.8	0.3	1.1	2.714
405.3	0.4	1.3	2.771
410.2	0.5	1.8	2.711
415.6	1.1	1.2	2.702
419.8	0.7	1.5	2.717
424.7	0.4	1.1	2.734
429.5	7.2	1.4	2.732
434.8	0.5	1.0	2.713
439.5	2.1	0.7	2.664
444.3	1.5	1.2	2.669
449.3	5.7		2.661
454.5	2.1	1.2	2.710
464.2	1.0	7.2	2.732
469.0	0.5	1.0	2.664
474.5	0.4	0.7	2.826
479.6	0.5	0.8	2.744
489.1	1.1	1.2	2.607
493.7	2.1	1.4	2.668
498.0	1.8	1.2	2.685

Table 6-14: Chemical analyses from carbonates in KSL-02.

Depth (m)	CaO %	MgO %	CaCO3 (%)	MgCO3 (%)
335.00	45.55	2.16	81.28	4.52
350.7	29.31	19.37	52.30	41.27
374.9	28.48	18.79	50.82	39.31
404.50	49.64	2.19	88.57	4.58
440.80-441.10	48.48	0.95	86.50	1.99
452.20 452.35	46.58	0.54	83.11	1.13
476.55-476.75	24.67	6.97	44.02	14.58

This page intentionally left blank

Daalsesingel 1
3511 SV Utrecht
scan@ebn.nl
www.scanaardwarmte.nl

Onderzoek in de ondergrond voor aardwarmte